

## DYNAMIC ERROR ANALYSIS OF SMART ELECTRICITY METER UNDER COMPLEX FLUCTUATING LOAD

Jingxia CHEN<sup>1</sup>, Kun LIU<sup>2,\*</sup>, Lijuan DU<sup>3</sup>

*Power Fluctuating of high-power loads in the power grid exerts impacts in different levels on Smart Electricity Meters (SEM), and even causes significant errors. In order to analyze the dynamic error sources of SEM, this paper adopted the method of mechanism modeling to establish dynamic mathematical models of the voltage channel, the current channel with Programmable Gain Amplifier (PGA) gain feedback control, the active power measurement unit, and the power measurement unit, respectively, and to structure the system-wide model of SEM. Then, a dynamic error model was built to study the impact of model parameters of each unit on the dynamic error of active electric energy, so as to trace the measurement error source of SEM for high-power loads. Using the error model, a PGA gain control algorithm based on sample point analysis was designed to optimize the PGA gain control unit model. Theory and simulation example proved that the system-wide model proposed in this paper can be employed to analyze the internal error influencing of electric energy meters under dynamic conditions and identify the source of error. The comparison of simulation results showed that the proposed proved PGA gain control algorithm can significantly reduce the measurement error of SEM for high-power loads. The research results in this paper can provide quantitative decision-making reference for improving the dynamic performance of SEM in the future.*

**Keywords:** dynamic error, smart electricity meter, error model, system-wide model

### 1. Introduction

In recent years, dynamic and unsteady features have steadily increased owing to the intermittent energy and large power electrical dynamic loads used in Smart Electricity Meters (SEMs). Dynamic error testing shows that the SEMs which are certified as qualified in steady condition may not necessarily meet the measurement error requirements in unsteady condition and some even have serious errors [1-2]. Therefore, study on the causes of non-ignorable errors during the dynamic testing is of great necessity.

<sup>1</sup> Ph.D. eng., Applied Science and Technology College, Beijing Union University, China

<sup>2</sup> A.P., Corresponding author, Applied Science and Technology College, Beijing Union University, China, e-mail: liu\_kun80@126.com

<sup>3</sup> Ph.D. eng., Applied Science and Technology College, Beijing Union University, China

Last decades have witnessed the significant development on error analysis of Smart Electricity Meter (SEM). Many studies have been conducted, including the accuracy of meters in real-world harmonic/inter-harmonic voltage and current conditions [3-5], the aspects related to the metrological characterization of meters under wide-range frequency deviations [6-8]. Correct estimation of four parameters of amplitude, phase, frequency and active power of fundamental and harmonic signals has been made by using Adaptive Measuring method, Amplitude-phase-locked Loop method, Gradient Descent Method etc. [9-11]. However, it should be pointed out that, so far, almost all meters' error analysis has been specifically considered in stationary situation with or without harmonics, and the used methods are suitable for frequency analysis, instead of time analysis.

In recent years, the dynamic error testing of smart electricity meters has begun to be noticed and received great attention from scholars, and some of them have achieved significant research results. In order to simulate actual dynamic power loads in smart grid, an on-off-keying testing dynamic current model was built with an OOK testing dynamic load energy model [12]. Furthermore, a distorted m-sequence dynamic test signal model was constructed to analyze the typical inherent characteristics of high-power power loads [13]. In addition, for evaluating the influence of signal waveforms, non-sinusoidal signal with five sets of harmonic components has been proposed to test electricity meters errors under the IEC 62053-21 standard [14-17].

As elaborated above, some error test signals and devices have been constructed to detect the dynamic error characteristics of electricity meters. However, there are few analyses on the error sources and internal error models of electric energy meters under fluctuating loads. Some scholars, by using algorithms instead of steady-state models, have established active power measurement algorithms for power measurement units under synchronous, quasi synchronous, and asynchronous sampling to analyze the steady-state error of the unit [18-20]. For electrical energy measurement units, some scholars have analyzed the conversion relationship between the accumulation of active power pulses and electrical energy [21-23]. Unfortunately, when exploring the error source, the problem has become quite complex because the existing dynamic error testing methods just focus on error without tracing [24-26].

In this research, we established an inner unit model including programmable gain Amplifier (PGA), Power Measuring, and Energy Measuring, and deduced a system-wide model by integrating those unit models. Then, we decomposed all errors, and traced to each unit after analyzing the dynamic error models. At last, a proved PGA gain control algorithm was proposed to reduce the measurement error of SEM for high-power fluctuating loads.

## 2. The dynamic model of Smart Electricity Meter

### 2.1 System block diagram of the electrical energy measuring module

The structure of active electrical energy measuring module in a SEM is shown in Fig.1, which is divided into four parts: Voltage input unit, Current input unit, Active power measurement unit, and Electrical energy measurement unit. First, the discrete voltage signal  $\{u(n): n \in N\}$  and the discrete current signal  $\{i(n): n \in N\}$  are obtained through PGAs and analog-to-digital converters (ADCs).

Second, the active power signal  $p_o(n)$  is calculated by multiplying  $u(n)$  and  $i(n)$ . And last, the electrical energy measurement unit realizes the accumulation of power over time, and therefore, obtain the accumulated energy signal  $e_o(n)$ .

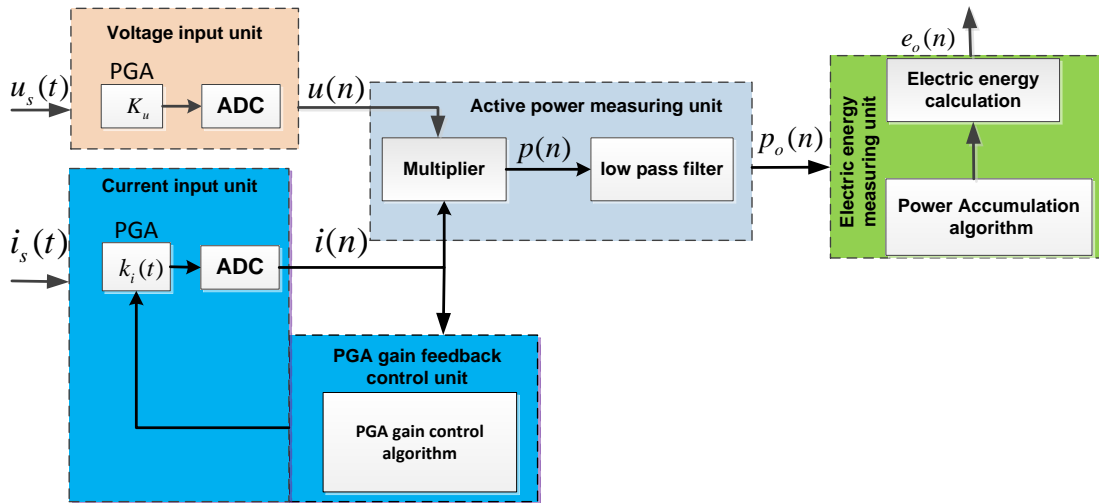


Fig. 1 Block Diagram of Energy Metering Module in SEM

### 2.2 Dynamic model of signal conversion unit

In the actual grid, there is a smaller amplitude variation range of AC voltage from the power load measurement port under the unsteady load condition when compared with current input unit. Therefore, the discrete output signal of Voltage input unit can be expressed as

$$u(n) = u_s(t) \Big|_{t=nT_s} \times K_u \quad (1)$$

in which  $K_u$  is fixed gain of PGA in voltage input unit,  $T_s$  is the ADC sampling interval.

On the contrary, the fluctuating load current amplitude range is larger in the actual grid. Therefore, the PGA gain must be adjusted to ensure the accuracy of the ADC measurement. Taking three ranges as examples, set the corresponding

PGA gain in Current input unit as  $K_{i1}$ ,  $K_{i2}$  and  $K_{i3}$ , and  $K_{i1} < K_{i2} < K_{i3}$  respectively, where  $K_{i1}$  is used for large amplitude current signals,  $K_{i2}$  for medium amplitude current signals, and  $K_{i3}$  for the small amplitude current signals. The PGA gain automatic switching process is shown in Fig. 2.

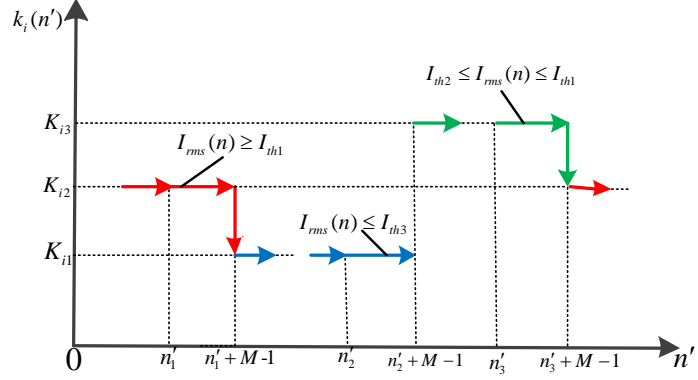


Fig. 2 Automatic adjusting process of PGA gain in Current input unit

In this figure,  $I_{th1}$ ,  $I_{th2}$  and  $I_{th3}$  are the corresponding current signal thresholds for  $K_{i1}$ ,  $K_{i2}$  and  $K_{i3}$ . Analysis shows that the PGA gain switching and the magnification do not adjust immediately along with the change of  $I_{rms}(n)$  and always lags  $M$  fundamental wave periods response, so when the current signal changes frequently, the dynamic error caused cannot be ignored.

According to the definition of the current RMS value, the dynamic current RMS  $\tilde{I}_{rms}(n')$  can be obtained by the following formula.

$$\tilde{I}_{rms}(n') = I_{rms}(N_T n) = \sqrt{\frac{1}{N_T} \sum_{k=0}^{N_T-1} i^2(N_T n - k)} \quad (2)$$

Thus, the dynamic gain value  $\tilde{k}_i(n')$  can be expressed recursively as

$$\tilde{k}_i(n') = \begin{cases} K_{i1}, \min \left\{ \tilde{I}_{rms}(n'): n' = n', n'-1, \dots, n'-M+1 \right\} \geq I_{th1} \\ K_{i3}, \max \left\{ \tilde{I}_{rms}(n'): n' = n', n'-1, \dots, n'-M+1 \right\} \leq I_{th3} \\ K_{i2}, I_{th2} \leq \left\{ \tilde{I}_{rms}(n'): n' = n', n'-1, \dots, n'-M+1 \right\} \leq I_{th1} \end{cases} \quad (3)$$

Therefore, the discrete dynamic current signal can be expressed as

$$i(n) = i_s(t)|_{t=nT_s} \times k_i(t)|_{t=nT_s} = i_s(n) \times k_i(n) = i_s(n) \times \tilde{k}_i(n')|_{n'=\left\lfloor \frac{n}{N_T} \right\rfloor} \quad (4)$$

Where  $\lfloor \cdot \rfloor$  is said to be rounded down.

### 2.3 Time domain dynamic model of active power measurement unit

Before analyzing, a few symbols are defined as follows.

$$\begin{aligned}\mathbf{U}_{n,k_1} &= [u(n), u(n-1), \dots, u(n-k_1+1)]^T \\ \mathbf{I}_{n,k_1} &= [i(n), i(n-1), \dots, i(n-k_1+1)]^T \\ \mathbf{P}_{n,k_1} &= [p(n), p(n-1), \dots, p(n-k_1+1)]^T \\ \tilde{\mathbf{P}}_{n-1,k_2} &= [p_o(n-1), p_o(n-2), \dots, p_o(n-k_2)]^T\end{aligned}$$

Where  $n$  represents the starting sequence number,  $k_1 (\in N)$ ,  $k_2 (\in N)$  represents the column vector dimension.

According to the linear shift invariant (LSI) system definition and the above mentioned definitions,  $p_o(n)$  must be expressed as a linear combination of Q-dimensional input vector  $\mathbf{P}_{n,q}$  and M-dimensional input vector  $\tilde{\mathbf{P}}_{n-1,m}$ ,

$$p_o(n) = -\mathbf{A}\tilde{\mathbf{P}}_{n-1,m} + \mathbf{B}\mathbf{P}_{n,q} \quad (5)$$

Where  $\mathbf{A} = [a_1, \dots, a_m]$ ,  $\mathbf{B} = [b_0, b_1, \dots, b_{q-1}]$ .  $\mathbf{P}_{n,q}$  is expressed as the Hadamard product form  $\mathbf{P}_{n,q} = \mathbf{U}_{n,q} \odot \mathbf{I}_{n,q}$  of column vectors  $\mathbf{U}_{n,q}$  and  $\mathbf{I}_{n,q}$ . Then

$$p_o(n) = -\mathbf{A}\tilde{\mathbf{P}}_{n-1,m} + \mathbf{B}[\mathbf{U}_{n,q} \odot \mathbf{I}_{n,q}] \quad (6)$$

The Eq. (6) shows the time-domain dynamic model structure of the active power measurement unit, whose parameters will be determined in the next section.

Under the steady-state condition, the active power can be expressed as

$$P = \sum_{k=0}^{N_T} \lambda_k p(N_T - k) = \sum_{k=0}^{N_T} \lambda_k u(N_T - k) i(N_T - k) \quad (7)$$

where the parameter  $\lambda_k$  is determined by the specific algorithm.

For easy analyzing, Eq.(7) can be written in the form of vector:

$$P = \lambda_T (\mathbf{U}_{N_T, N_T+1} \odot \mathbf{I}_{N_T, N_T+1}) \quad (8)$$

where  $\lambda_T = [\lambda_0, \lambda_1, \dots, \lambda_{N_T}]$ . In Eq. (6), when  $n = N_T$ ,

$$p_o(N_T) = -\mathbf{A}\tilde{\mathbf{P}}_{N_T-1,m} + \mathbf{B}[\mathbf{U}_{N_T,q} \odot \mathbf{I}_{N_T,q}] \quad (9)$$

When the power measurement unit input is a dynamic signal, this research gives the model parameters  $\mathbf{A} = 0$ ,  $\mathbf{B} = \lambda$ ,  $q = L$ , where  $\lambda$  and  $L$  are adjustable. According to the filter theory, the power measurement unit model can be written in the form of the filter coefficient vector multiplied by the input vector.

$$p_o(n) = \mathbf{H}\mathbf{P}_{n,L} = \mathbf{H}[\mathbf{U}_{n,L} \odot \mathbf{I}_{n,L}] \quad (10)$$

Where  $L$  is the length of the low pass filter,  $\mathbf{H} = \lambda = [\lambda_0, \lambda_1, \dots, \lambda_{L-1}]$ . The power measurement unit model has been simplified to the Moving Average (MA) model, and its filter parameters are determined by the general form of the power

measurement algorithm in Eq. (7). Therefore, Eq.(10) is the General Moving Average (GMA) dynamic mode of the power measurement unit.

Taking the Complex Rectangle Algorithm as an example, the model of active power measurement unit will be changed to the following Rectangle-MA form.

$$p_o(n) = \mathbf{H}_R(\mathbf{U}_{n,L} \odot \mathbf{I}_{n,L}) \quad (11)$$

Where  $\mathbf{H}_R = [h_0, h_1, \dots, h_{L-1}]$ ,  $h_k = \begin{cases} \frac{1}{L-1}, & k = 1, 2, \dots, L-1 \\ 0, & k = 0 \end{cases}$ .

## 2.4 System-wide dynamic model

The active electrical energy measurement signal  $e_o(n)$  is defined as,

$$e_o(n) = \sum_{k=0}^n p_o(k) T_s \quad (12)$$

According to formula (10), there are  $p_o(k) = \mathbf{H} \mathbf{P}_{k,L} = [h_0, h_1, \dots, h_{L-1}] \begin{bmatrix} p(k) \\ p(k-1) \\ \vdots \\ p(k-L+1) \end{bmatrix}$ ,  $k \in [0, n]$ .

By integrating the dynamic models of SEM, we can derive system-wide model of smart meter measurement module.

$$e_o(n) = T_s \sum_{k=0}^n \mathbf{H} \mathbf{P}_{k,L} = \mathbf{H} \begin{bmatrix} T_s \sum_{k=0}^n p(k) \\ T_s \sum_{k=0}^{n-1} p(k) \\ \vdots \\ T_s \sum_{k=0}^{n-L+1} p(k) \end{bmatrix} = T_s \mathbf{H} \begin{bmatrix} \sum_{k=0}^n u(k)i(k) \\ \sum_{k=0}^{n-1} u(k)i(k) \\ \vdots \\ \sum_{k=0}^{n-L+1} u(k)i(k) \end{bmatrix} = T_s \mathbf{H} \begin{bmatrix} \sum_{k=0}^n k_u \tilde{k}_i(n') u_s(i) i_s(t) \\ \sum_{k=0}^{n-1} k_u \tilde{k}_i(n') u_s(i) i_s(t) \\ \vdots \\ \sum_{k=0}^{n-L+1} k_u \tilde{k}_i(n') u_s(i) i_s(t) \end{bmatrix}_{t=kT_s, n' = \left\lfloor \frac{k}{N_T} \right\rfloor} \quad (13)$$

On the basis of the dynamic internal models of electrical energy measuring module and the system-wide dynamic model, the following analysis will present the influences caused by model parameters of each unit on the instantaneous active power signal.

## 3. Error analysis of SEM under fluctuating load

Fluctuating Load refers to the electrical load that uses rapidly changing power from the grid during production periodically or randomly, such as high-speed railway locomotive, steelmaking electric arc furnace, steel rolling mill, etc.

The most obvious characteristic of high-power fluctuating load is that the amplitude of current signal changes randomly with a wide range. Studying on the dynamic models described in Section 2, it is found that when the amplitude of current input signal changes randomly within a large range, there is a sensitive reaction of the current input unit and less error of power measurement unit and electric energy measurement. Accordingly, this research focuses on analyzing the dynamic error of current input channel with PGA module.

In order to avoid the frequent mis-switching of the range caused by periodic interference, the PGA gain switching is often delayed by the cycle in an actual smart meter design. That is, when the amplitude of the grid current changes, the PGA gain at the same time will not change immediately, but remains for a period of time. This can result in power grid current signal being incorrectly amplified or deviating from the optimal sampling range of the ADC, which can lead to errors in power metering at a later stage.

A simulation is quoted below to describe the measurement error caused by PGA gain switching delay in detail. As shown in Fig. 3, the grid current signal maintains a small signal amplitude in 1~2 fundamental periods. When the current signal amplitude increases rapidly from the third period, it lasts for 10 periods, and then returns to a small amplitude signal from the 13th period. According to the principle of choosing small gain for large amplitude signal, the signal within 3~12 periods should be chosen as a small gain. However, because the PGA gain switching lags  $M$  periods, the large amplitude signal in the 3~(3+ $M$ ) periods is limited. Similarly, the small amplitude signal in the 13~(13+ $M$ ) period deviates from the optimal sampling range of ADC due to insufficient PGA gain.

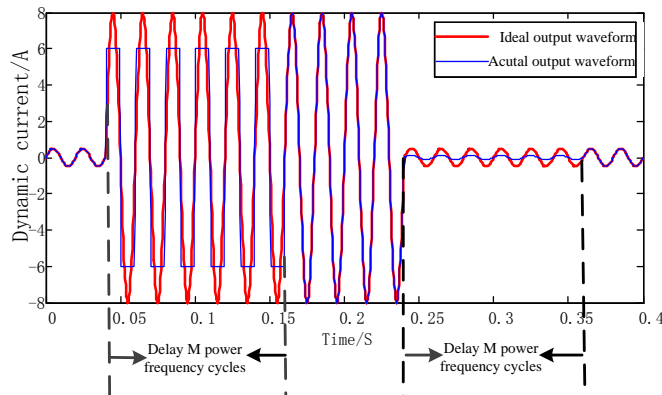


Fig. 3 An example of PGA gain switching delay

From the above analysis, it can be seen that the greater the  $M$  value or the more frequent the rapid fluctuation of the current value, the greater the difference between the output signal of the current channel and the actual current input signal, the greater the measurement error of the active power and electric energy

caused by this; However, the  $M$  value is too small, which may lead to frequent mis-switching of the PGA gain caused by periodic interference.

The influence of lag period on error is analyzed theoretically. Assume that during the initial stage of measurement (within the  $0 \sim N_1 T_1$  time period), the voltage divider of the electric energy meter outputs a steady state voltage signal with an effective value of  $U$  (V), and the shunt of the electric energy meter outputs a steady state current signal with a small effective value of  $I_0$  (A). To ensure that the signal is within the reasonable measurement range of ADC, the current PGA will choose a larger gain value of  $K_0$ . When other error factors are not considered, the active electric energy is:

$$E_0 = UK_0 I_0 \cos \varphi \cdot t / K_0 = UI_0 \cos \varphi \cdot t \quad (14)$$

It is the same as the electric energy value obtained by ideal operation, so it can be said that the error caused by PGA gain amplification under steady-state conditions is approximately 0.

However, when the amplitude of the current signal changes suddenly, it is assumed that the effective value increases to  $K_i I_0$  (A) during the  $N_1 T_1 \sim N_2 T_1$  time period. Ideally, the gain value of PGA will decrease to  $K_0 / K_i$  to accommodate the dynamic transformation of the input signal. However, in practical application, the gain change of current PGA will lag behind the  $M$  fundamental periods ( $T_1$ ), which means that the indication value of current signal will still be amplified to  $K_i K_0 I_0$  within the  $M$  fundamental periods. When it is larger, the current signal amplitude  $\sqrt{2} K_i K_0 I_0$  will exceed the ADC range  $\pm M_a$ , causing the current signal to be limited. Assuming that the reading of active power in the time period is reduced to  $P_M$  % of active power in the  $0 \sim N_1 T_1$  time period, without considering other error factors, the active electric energy in the  $N_1 T_1 \sim N_1 T_1 + M T_1$  time period is

$$E_1 = \frac{UK_i K_0 I_0 P_M \% \cos \varphi \cdot M T_1}{K_0} = UK_i I_0 P_M \% \cos \varphi \cdot M T_1 \quad (15)$$

therefore, the actual measured active electric energy in the  $N_1 T_1 \sim N_2 T_1$  time period is

$$E_x = E_1 + UK_i I_0 \cos \varphi \cdot (N_2 - N_1 + M) T_1 \quad (16)$$

then the corresponding active electric energy error is

$$\begin{aligned} \Delta E_x &= \frac{E_x - E_0}{E_0} \cdot 100\% \\ &= \frac{UK_i I_0 P_M \% \cos \varphi \cdot M T_1 + UK_i I_0 \cos \varphi \cdot (N_2 - N_1 + M) T_1 - UK_i I_0 \cos \varphi \cdot (N_2 - N_1) T_1}{UK_i I_0 \cos \varphi \cdot (N_2 - N_1) T_1} \cdot 100\% \quad (17) \\ &= \frac{(1 + P_M \% M)}{N_2 - N_1} \cdot 100\% \end{aligned}$$

In the above formula,  $E_o = UK_i I_0 \cos \varphi (N_2 - N_1)T_1$  is the theoretical reference value of active electric energy in the  $N_1 T_1 - N_2 T_1$  time period.

According to the analytical formula (17), decreasing the value of  $M$  or increasing the measurement time can reduce the dynamic error caused by the range switching delay. Considered together, the value of  $M$  should be 3~4, which can greatly reduce the dynamic error and avoid the wrong PGA gain switching caused by interference. At the same time, the lag period  $M$  of switching from large gain to small gain and from small gain to large gain should be basically equal, so that the dynamic error can be compensated.

#### 4. A Design for Reducing PGA Dynamic Error

To solve the technical problem that the analog current signal  $i_s(t)$  exceeds the current range of ADC module after being amplified by PGA module, this research designs a PGA gain control algorithm based on sampling point analysis.

Theoretical and simulation analysis shows that the current signal amplitude can be determined by the corresponding limited amplitude interval time. As shown in Fig. 4(a)~4(d),  $I_M$  is the maximum current measurement value of ADC module, and  $T_s$  is its sampling period.

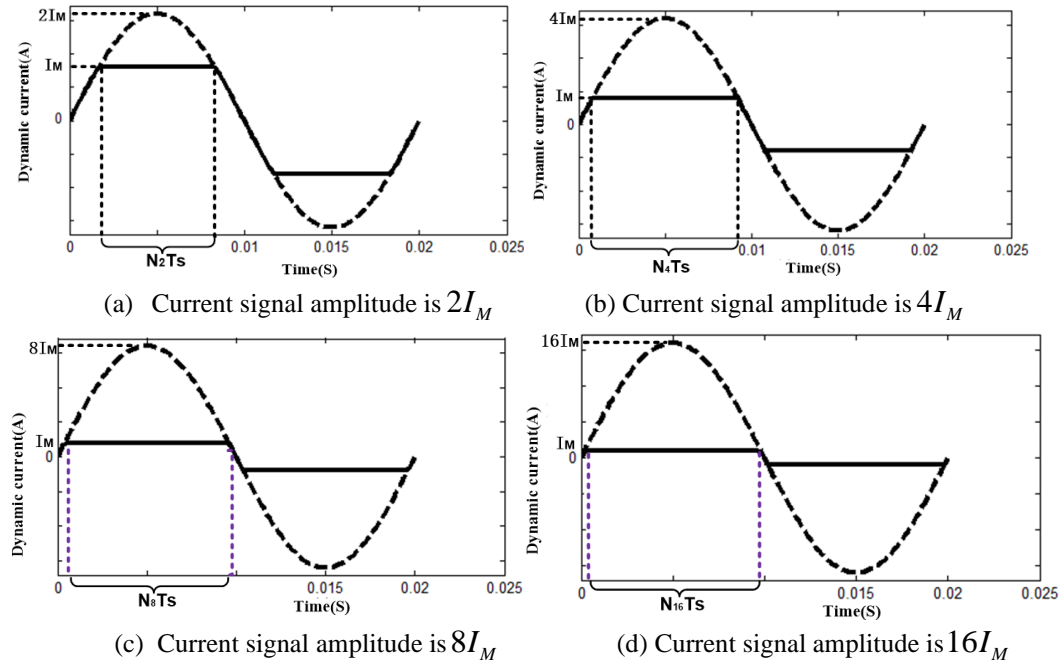


Fig. 4 Schematic diagram of the number of integer multiple limited amplitude sampling points

When the current signal amplitude increases to  $2 I_M$ ,  $4 I_M$ ,  $8 I_M$  and  $16 I_M$ ,  $N_2 T_s$ ,  $N_4 T_s$ ,  $N_8 T_s$ ,  $N_{16} T_s$  are respectively defined as the interval time of all sampling points exceeding  $I_M$  during a fundamental wave period.

The simulation implementation steps for the sampling point analysis algorithm are as follows.

Step1. Set the amplitude of the current input signal to be 2,4,8,16 times of  $I_M$ , and record the number of sampling points  $N_2$ ,  $N_4$ ,  $N_8$ ,  $N_{16}$  that exceed  $I_M$  during simulation.

Step2. Set any value between  $2I_M$  and  $16I_M$  as the input signal for simulating the actual current, and record the number of sampling points exceeding  $I_M$  as  $N_C$  during a fundamental wave period.

Step3. Conduct comparative analysis. It shows that when  $N_2 \leq N_C < N_4$ , the current signal amplitude is 2~4 times of  $I_M$ , so the gain amplification factor  $k_i$  of PGA module should be reduced by 4 times to ensure that the actual current signal amplitude is within the optimal sampling range of ADC; Similarly, when  $N_4 \leq N_C < N_8$ , the gain amplification factor  $k_i$  should not be more than  $I_M / 8$ ; when  $N_8 \leq N_C < N_{16}$ , the gain amplification factor  $k_i$  should not be more than  $I_M / 16$ .

Step4. Feedback the factor  $k_i$  obtained from the analysis in Step3 to the PGA module.

## 5. Algorithm verification

To verify the new algorithm, our project team constructed a system-wide model of SEM [12] and added the sampling point analysis algorithm to it. The specific installation diagram is shown in Fig5.

In the verification experiment, an actual certain SEM was selected as the tested meter, and the Complex Rectangle Algorithm was applied to its power measurement. The dynamic error test results and new algorithm simulation results under transient, short-term, and long-term dynamic load modes[12] are shown in Table 1. It is obvious that after using the new algorithm, the dynamic error of the electricity meter is much smaller than before use.

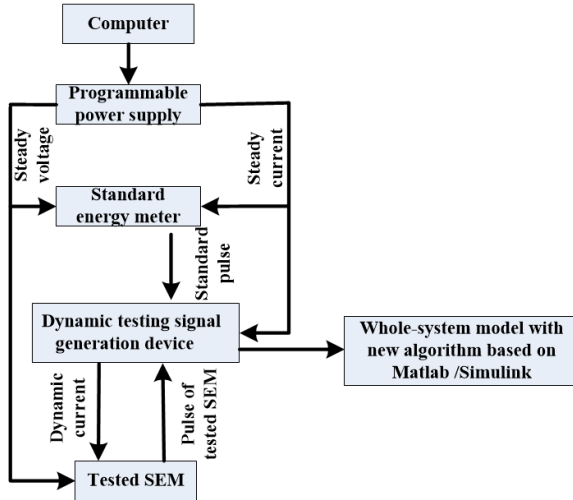


Fig.5 Schematic installation diagram for algorithm verification

Table 1.

New algorithm verification results		
On:Off	Tested error (%)	Simulation error after using new algorithm (%)
20:100	-57.67	-7.98
30:80	-38.01	-5.32
40:40	-33.9	-3.99
40:100	-30.61	-3.63
80:200	-16.08	-2.01
300:300	-5.92	-0.53

## 6. Conclusions

In this research, a mathematical model of SEMs' voltage channels, current channels with PGA, active power measurement units, and dynamic models of electric energy measurement units were constructed to track the source of dynamic error. In addition, a comprehensive system-wide model was established based on the internal signal transmission relationship of SEM. By comparing the dynamic error of experimental testing with the simulation analysis results, it was shown that the system-wide model SEM established can be employed to better analyze the source of dynamic error. Furthermore, in order to reduce the dynamic measurement error, a proved PGA gain control algorithm was proposed for high-power loads. Applying the new PGA unit gain control algorithm, PGA switching

time was greatly reduced and mis-operation was also reduced. As for the time relationship, this research only focuses on the optimization algorithm for PGA dynamic switching that caused the largest dynamic error, and the optimization analysis for other units needs to be further carried out. However, the results of this study can not only provide an important basis for improving the dynamic measurement performance of smart meters, but also play an important guiding role in improving the algorithm of metering chips, optimizing the overall design of SEMs, and selecting electric energy meters for power departments in the case of fluctuating load.

### Acknowledgments

This work is supported by the General projects of science and technology plan of Beijing Municipal Education Commission (KM202111417002) and the Scientific Research Project of Beijing Union University (Zk30201902).

### R E F E R E N C E S

- [1] *Van D, Leeuwen R V, Marais Z, et al*, “EMC Testing of Electricity Meters Using Real-World and Artificial Current Waveforms”, *IEEE Transactions on Electromagnetic Compatibility*, **vol. 63**, no. 6, 2021, pp. 1865-1874.
- [2] *Bejan I, Jensen C L, Andersen L M, et al*, “Inducing flexibility of household electricity demand: The overlooked costs of reacting to dynamic incentives”, *Applied Energy*, **vol. 284**, 2021.
- [3] *C. J. Chou and C. C. Liu*, “Analysis of the performance of induction watthour meters in presence of harmonics”, *Electric Power Syst. Res.*, **vol. 32**, no. 1, 1995, pp. 71-79.
- [4] *Durante L G, Ghosh P K*, “Active power measurement in nonsinusoidal environments”, *IEEE Transactions on Power Systems*, **vol. 15**, no. 3, 2000, pp. 1142-1147.
- [5] *Diahovchenko I, Volokhin V, Kurochkina V, et al*, “Effect of harmonic distortion on electric energy meters of different metrological principles”, *Frontiers energy*, **vol. 13**, no. 2, 2019, pp. 377-385.
- [6] *Vincenzo, Paciello, Antonio, et al*, “Smart Sensors for Demand Response”, *IEEE Sensors Journal*, **vol. 17**, no. 23, 2019, pp. 7611-7620.
- [7] *Cataliotti A, Cosentino V, Nuccio S*, “Static Meters for the Reactive Energy in the Presence of Harmonics: An Experimental Metrological Characterization”, *IEEE Transactions on Instrumentation & Measurement*, **vol. 58**, no. 8, 2009, pp. 2574-2579.
- [8] *Femine A D, Gallo D, Landi C, et al*, “Advanced Instrument For Field Calibration of Electrical Energy Meters”, *IEEE Transactions on Instrumentation & Measurement*, **vol. 58**, no. 3, 2009, pp. 618-625.
- [9] *Xia X, Yang X, Liang W*, “ABSI: An Adaptive Binary Splitting Algorithm for Malicious Meter Inspection in Smart Grid”, *IEEE Transactions on Information Forensics and Security*, **vol. 14**, no. 2, 2019, pp. 445-458.
- [10] *Xin, Wang, Edwin, et al.*, “Smart Power Grid Synchronization with Fault Tolerant Nonlinear Estimation. *IEEE Transactions on Power Systems*”, **vol. 31**, no. 66, 2016, pp. 4806-4816.

- [11] *Avdar S H, Feryad V*. “Efficient Design of Energy Disaggregation Model with BERT-NILM Trained by AdaX Optimization Method for Smart Grid”, *Energies*, **vol. 14**, no. 15, 2021, pp. 4649.
- [12] *Wang X, Chen J, Yuan R, Jia X, Zhu M, Jiang Z*, “OOK power model based dynamic error testing for smart electricity meter”, *Meas Sci Technol*, **vol. 28**, no. 2, 2017, pp. 025015-025022.
- [13] *Wang X, Wang J, Wang L, et al*, “Non-overlapping moving compressive measurement algorithm for electrical energy estimation of distorted m-sequence dynamic test signal”, *Applied Energy*, **vol. 251**, no. 2, 2019, 113234.
- [14] *Munehiko K, Hayo Z, Oliver H*, “Applicability of a Commercially Available Active Extremity Dose-Rate Meter to Eye Lens Dose Monitoring”, *Radiation Protection Dosimetry*, **vol. 192**, no. 4, 2020, pp. 460-472.
- [15] Electricity metering equipment (a.c.) general requirements, tests and test conditions-part 11: Metering equipment IEC EN 62052-11. March 2003.
- [16] *Georgakopoulos D, Wright PS*, “Exercising the dynamic range of active power meters under nonsinusoidal conditions”, *IEEE Trans Instrum Meas*, **vol. 56**, no. 2, 2007, pp. 362-372.
- [17] *Gallo D, Landi A, Pasquino N, Polese N*, “A new methodological approach to quality assurance of energy meters under nonsinusoidal conditions”, *IEEE Trans Instrum Meas*, **vol. 56**, no. 5, 2007, pp. 694-702.
- [18] *Nguyen T K, Dekneuvel E, Jacquemod G, et al*, “Development of a real-time non-intrusive appliance load monitoring system: An application level model”, *International Journal of Electrical Power & Energy Systems*, **vol. 90**, 2017, pp. 168-180.
- [19] *Ren H, Hou Z, Vyakaranam B, et al*, “Power System Event Classification and Localization Using a Convolutional Neural Network”, *Frontiers in Energy Research*, 2020.
- [20] *Cao S, Xu J, Miao Z, et al*, “Steady and transient operation of an organic Rankine cycle power system”, *Renewable energy*, **vol. 133**, 2019, pp. 284-294.
- [21] *Jrventausta P, Repo S, Rautiainen A, et al*, “Smart grid power system control in distributed generation environment”, *IFAC Proceedings Volumes*, **vol. 42**, 2009, no. 9, pp. 10-19.
- [22] *Cossent R, Gomez T, Olmos L*, “Large-scale integration of renewable and distributed generation of electricity in Spain: Current situation and future needs”, *Energy Policy*, **vol. 39**, no. 12, 2011, pp. 8078-8087.
- [23] *Dogan A*, “Real-time demand response of thermostatic load with active control”, *Electrical engineering*, **vol. 100**, no. 4, 2018, pp. 2649-2658.
- [24] *Wang X, Wang J, Yuan R, et al*, “Dynamic error testing method of electricity meters by a pseudo random distorted test signal”, *Applied Energy*, **vol. 249**, 2019, pp. 67-78.
- [25] *Fekri M N, Patel H, Grolinger K, et al*, “Deep Learning for Load Forecasting with Smart Meter Data: Online Adaptive Recurrent Neural Network”, *Applied Energy*, **vol. 282**, No.3, 2020, pp.116-177.
- [26] *Cetina R Q, Seferi Y, Blair S M et al*, “Energy Metering Integrated Circuit Behavior beyond Standards Requirements”, *Energies*, **vol. 14**, No.2, 2021, pp.390-409.